Comparison of Histogram-based Textural Features between Cancerous and Normal Prostatic Tissue in Multiparametric Magnetic Resonance Images

Comparison of Histogram-based Textural Features between Cancerous and Normal Prostatic Tissue in Multiparametric Magnetic Resonance Images

B. De Santi, M. Salvi, V. Giannini, K. M. Meiburger, F. Marzola, F. Russo, M. Bosco and F. Molinari

***Abstract*— In the last decade, multiparametric magnetic resonance imaging (mpMRI) has been expanding its role in prostate cancer detection and characterization. In this work, 19 patients with clinically significant peripheral zone (PZ) tumours were studied. Tumour masks annotated on the whole-mount histology sections were mapped on T2-weighted (T2w) and diffusion-weighted (DW) sequences. Gray-level histograms of tumoral and normal tissue were compared using six first-order texture features. Multivariate analysis of variance (MANOVA) was used to compare group means. Mean intensity signal of ADC showed the highest showed the highest area under the receiver operator characteristics curve (AUC) equal to 0.85. MANOVA analysis revealed that ADC features allows a better separation between normal and cancerous tissue with respect to T2w features (ADC: P = 0.0003, AUC = 0.86; T2w: P = 0.03, AUC = 0.74). MANOVA proved that the combination of T2-weighted and apparent diffusion coefficient (ADC) map features increased the AUC to 0.88. Histogram-based features extracted from *in-vivo* mpMRI can help discriminating significant PZ PCa.**

I. Introduction

Prostate cancer (PCa) is the second-most common cancer worldwide, with 1,276,106 new cases registered in 2018 [1]. The standard technique for the diagnosis and grading of PCa is the analysis of the histological specimen. However, the collection of one or more histological samples is invasive and allows to analyze only a small portion of the prostate volume.

In the last decade, multiparametric magnetic resonance imaging (mpMRI), i.e. the integration of a structural MR sequence such as T2-weighted (T2w) with a functional one such as diffusion-weighted (DW), has emerged as a promising tool for the non-invasive detection and characterization of PCa. In T2w images, tumours in the peripheral zone (PZ), which represent the 70-80% of prostate tumours [2], appear as masses with lower signal intensities (SI) as they present high cellular density [2]. However, this modality exhibits a high false-positive rate since even other pathological conditions, such as prostatitis or haemorrhage, show image features similar to a cancerous area [2]. DW images are used to reconstruct apparent diffusion coefficient (ADC) maps which quantify the diffusion of water molecules through the tissue. Due to high cellular density, cancerous tissue is characterized by restricted diffusion, therefore tumours show lower ADC values with respect to normal tissue. Unfortunately, DW images suffer from geometrical distortion due to the echo-planar imaging Recent studies showed that the combination of these two MR modalities (T2w and DW) improve the accuracy in PCa diagnosis with respect to single MR modalities [3,4].

Texture analysis is a technique able to extract quantitative features describing the appearance of digital images in terms of homogeneity, regularity and coarseness. In medical imaging, these features were often used as imaging *biomarkers* associated with the presence of pathological conditions. In the particular context of MR prostate cancer, Madhabushi et al. [5] developed a computer-aided detection (CAD) system for prostate cancer detection in 3D *ex-vivo* T2w images using first-order textural features which describe the gray-level histogram and Haralick features which measure heterogeneity in terms of spatial patterns of pixel with the same gray-level. In [4], first-order features, Haralick features, and pharmacokinetic parameters were extracted from T2w, DW and dynamic contrast-enhanced (DCE) *in-vivo* images of PZ PCa for discrimination between normal and cancerous tissue. Further, texture features extracted from T2w and ADC images also showed significant differences between cancerous tissuewith different aggressiveness grading [3]. Other studies analyzed the histogram of PZ lesions in ADC maps to predict patient prognosis [6]. Anyway, in these studies, no in-depth investigation has been made about which texture features mostly contribute to discrimination of normal and pathological tissue in a multiparametric framework.

The aim of this paper was to investigate differences in histogram-based textural features between tumoral and normal tissue in T2w and ADC images of PZ PCa. Multivariate analysis was performed in order to evaluate diagnostic performance of the combination of T2w and ADC first-order features.

II. Materials and Methods

A. Patients and inclusion criteria

In this study, all individuals complied with the following four inclusion criteria were enrolled: (a) biopsy-proven prostate adenocarcinoma (b) mpMRI examination between September 2017 and February 2019, including axial DW and T2w imaging, (c) radical prostatectomy within 2 months of MRI, and (d) a significant peripheral zone (PZ) lesion greater than 0.5 ml in the whole-slide histological sample. The study was approved by the local Ethics Committee and all the participants signed an informed consent form. The population

B. De Santi, M. Salvi, K.M. Meiburger, F. Marzola and F. Molinari are with the PoliTo BIO^{Med} Lab, Department of Electronics and Telecommunications, Politecnico di Torino, Turin, Italy. (corresponding author to provide e-mail: bruno.desanti@polito.it).

V. Giannini and F. Russo are with the Candiolo Cancer Institute, FPO-IRCCS, Candiolo, Turin, Italy. M. Bosco is with the Department of Pathology, San Lazzaro Hospital, Alba, Cuneo, Italy.

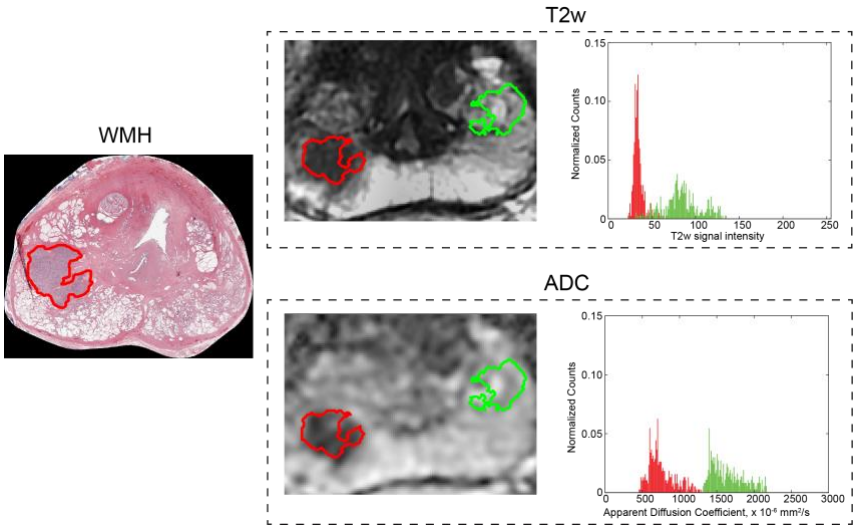

Figure 1. Starting from the whole-mount histological (WMH) slice, the cancerous area (red) was registered on the T2w image. Then, the healthy ROI was obtained by mirroring the tumor shape. Finally, histograms of the tumoral and normal tissue were extracted.

sample included 21 patients with single or multiple foci, for a total of 37 lesions. The histological grade (Gleason Group – GG) of the 37 PCa lesions were: 13 GG2, 13 GG3, 11 GG4.

B. Data acquisition protocol

MpMRI images were collected with a 1.5 T scanner (Signa Excite HD, GE Healthcare, USA) using a four-channel phased-array coil combined with an endorectal coil (Medrad, Indianola, USA). The following protocol was adopted to acquire the T2w images: slice thickness of 3 mm; TR/TE of 3020/85 ms; field of view equal to 16 × 16 cm; acquisition matrix of 384 × 288 with a reconstruction matrix of 512 × 512 pixels. DW images have been obtained with the same protocol except for TR/TE of 7000/101 ms; acquisition matrix of 128 × 128 with a reconstruction matrix of 256 × 256; b-values equal to 0 and 1000 s/mm^2. The prostate gland was segmented in T2w images by an expert radiologist (F.R), with 11 years of experience in MRI prostate examination.

Regarding the histological images, prostate specimen was step-sectioned at 3 mm intervals perpendicular to the long axis (apical-basal) of the gland. In this way, the inclination of axial T2w images (which were acquired perpendicular to the rear gland surface) was confidently reproduced. The histological tissues were sectioned into 5 µm slices, mounted onto adhesive slides, and stained with haematoxylin and eosin. An expert pathologist (M.B), with 15 years of experience in uropathology, manually outlined each clinically significant peripheral tumour on WMH slices.

C. ADC – T2w image registration

ADC maps were extracted from DW images, which were geometrically distorted due to the presence of susceptibility artifacts and the EPI sequence. In order to correct these distortions, the deformation field mapping the DW image with b-value = 0 to the T2w image was computed using an automatic algorithm developed by our research group [7]. The method consisted of three steps: i) automatic region-of-interest extraction; ii) physiological motion correction by affine transformation; iii) diffeomorphic Demons algorithm for non-linear geometric distortions. ADC maps were computed using the exponential model. Finally, ADC images were registered to the T2w images using the deformation field computed between the DW and T2w images.

D. WMH – T2w image registration

For each whole-mount histological (WMH) slice, the same pathologist (M.B.) and radiologist (F.R.) manually selected the corresponding T2w slice by visually identifying anatomical landmarks (e.g. urethra, ejaculatory ducts, adenomas).

In order to accurately localize the tumour in the MRI images, the WMH slice and the corresponding tumour masks were registered to the T2w image. To improve registration accuracy, a two-steps procedure was adopted: i) segmentation of the tissue in the WMH slice was segmented using an object-based detection algorithm and morphological operators; ii) T2w image cropping in a region including only the PG using the same algorithm described in [7] iii) annotation of approximately 20 corresponding points for each pair of images (WMH and T2w) in correspondence of identifiable anatomical landmarks (e.g. urethra, ejaculatory ducts, adenomas). The T2w cropped image and the red channel of the WMH slice were used as fixed and moving image, respectively. Elastix toolbox (version 4.9) was used to perform the nonrigid registration [8]. We chose a multi-metric and a multi-resolution registration approach: Mutual Information and Euclidean distance between corresponding points were chosen as metrics with equal weights; two pyramid levels. An affine transformation followed by a B-spline with grid spacing equal to 32 and 16 pixels were computed. Final registration parameters were tuned by minimizing the mean Euclidean distance between corresponding points.

F. Normal tissue region-of-interest definition

To assess the potential of textural features in discriminating cancerous and normal tissue, a region-of-interest (ROI) was automatically extracted in the T2w image by reflecting the tumour mask across the minor axis of an ellipse with the same second moment of the prostate gland mask (Fig.1). This reflected mask was then intersected with the prostate gland mask and, in case of multiple foci, all pixels in common with the tumour masks were excluded. This strategy allows to reduce bias in the texture analysis results due

to different sample sizes, zones and slices. The radiologist visually assessed the validity of the normal tissue ROI.

G. Texture analysis

Texture analysis was performed in the cancerous tissue and in the normal tissue in both T2w and ADC images. First-order textural features, which describe the gray-level distribution, were computed: Mean (M), Standard Deviation (SD), kurtosis (K), skewness (Sk), entropy (Ent) and energy (H). For entropy and energy calculation, we extracted the gray-level histogram using 256 levels, minimum and maximum values were set to the 1st percentile and 99th percentile of the gray-level values observed in the whole image dataset. Since the lack of standardized signal intensity values of morphological T2w images may bias texture analysis results, we chose to normalize the T2w signal intensities. Mean signal intensity of the obturator muscle was used as reference for T2w image normalization [9].

H. Statistical analysis

Mean and standard deviation values of features were computed for the two groups (normal tissue and cancerous tissue) and compared using a two-tailed paired t-test. One-way multivariate analysis of variance (MANOVA) was used to compare the two data groups and to compute the canonical variables, which are linear combinations of the original variables, that maximize the separations between groups. Three separate MANOVA analysis were performed using: i) T2w features; ii) ADC features and iii) T2w + ADC features. Belsley collinearity was used to assess sources of collinearity among variables in a multiple linear regression. All statistical tests were carried out with a significance level of 0.05. Finally, receiver operating characteristic (ROC) curve and area under the curve (AUC) were calculated for each texture feature and for the canonical variables of the MANOVA by simple cut-off analysis.

TABLE I. HISTOGRAM-BASED TEXTURAL FEATURES

Modality	*Feature*	*Normal tissue*	*Tumor*	*AUC*
T2w	M **	145.98 (67.42)	106.61 (52.75)	0.68
	SD **	43.38 (23.28)	27.71 (14.94)	0.71
	K	0.44 (0.67)	0.82 (0.66)	0.66
	Sk	3.25 (1.16)	4.20 (1.47)	0.68
	Ent **	5.26 (0.77)	4.67 (0.81)	0.71
	H *	0.04 (0.03)	0.06 (0.03)	0.71
ADC	M ***	1278.68 (297.17)	994.25 (291.26)	0.85
	SD	248.41 (90.23)	207.29 (64.45)	0.65
	K *	-0.07 (0.84)	0.29 (0.59)	0.64
	Sk	3.14 (1.43)	3.33 (0.85)	0.65
	Ent	5.92 (0.56)	5.88 (0.44)	0.58
	H	0.02 (0.01)	0.02 (0.01)	0.56

Measurement units of M and SD in ADC images are mm and 10^{-6} mm^2 /s, respectively. *, ** and *** indicate $P < 0.05$, $P < 0.005$ and $P < 0.0005$

III. RESULTS

For 7 out of 37 tumours, no correspondence between WMH and T2w slices could be established with enough confidence, hence, these cases were discarded for this study. Multiple foci were found in 8 patients (3 patients with 3 foci, 5 patients with 2 foci), the remaining 11 patients showed a single lesion. Summarizing, a total of 30 tumours from 19 patients, were analyzed. Mean Euclidean distance after WMH - T2w registration with optimal parameters was 2 ± 1.2 mm, where the mean equivalent diameter of the lesions was 9.3 ± 6.1 mm.

Mean and standard deviation values of features are reported in Table I. In T2w images, normal tissue had higher values of M (145.98 vs 106.61, $P < 0.005$), SD (43.38 vs 27.71, $P < 0.005$), Ent (5.26 vs 4.67, $P < 0.005$) while H was higher in tumoral tissue (0.04 vs 0.06, $P < 0.05$). Regarding ADC maps, M resulted to be statistically lower in tumoral tissue (1278.68 vs 994.25, $P < 0.0005$). Highest AUC value was yielded by M (0.85) in ADC. Fig. 1 shows an example of comparison of gray-level histograms between tumoral and normal tissue in T2w and ADC images.

Collinearity test highlighted multicollinearity among variables introduced by Ent in both ADC and T2w with a variance-decomposition proportion of in both modalities equal to 0.94. Indeed, Ent resulted to be correlated with SD and H in both modalities (T2w: Ent-SD 0.89, Ent-H 0.95; ADC: Ent-SD $r = 0.93$, Ent-H $r = 0.94$). After removing Ent, no collinearity was found. In each of the three experiments (only T2w features, only ADC features and the combination T2w + ADC), MANOVA dimension resulted to be 1 with $P < 0.05$ for T2w and $P < 0.005$ for ADC and ADC + T2w. Fig. 2a shows the scatter plot of the canonical variables resulting from MANOVA using the multiparametric features. Figure 2b shows the ROC curves for T2w, ADC and T2w + ADC. The combination T2w + ADC showed the highest AUC (88.33 compared with 74.33 for T2w and 85.89 for ADC).

IV. DISCUSSION AND CONCLUSIONS

Previous studies already showed that MR imaging has huge potential for PZ PCa detection and characterization [2].Several studies showed that the combination of different magnetic resonance modalities such as T2w, and DW, which is also known as mpMRI, improve the diagnostic accuracy of prostate cancer [2,3,4]. However, most studies have not analyzed and discussed which histogram-based feature was relevant in the differentiation between PZ tumoral and normal tissue when considering single or multiple modalities.

In this study, a total of 30 PZ tumours were described in terms of histogram-based features in *in-vivo* mpMRI images. Tumours were segmented in the WMH slice by an expert pathologist. The tumor masks were registered with the MR image by estimating an affine and a B-spline transformation between T2w and the WMH slice. The functional ADC maps were automatically registered to the morphological MR images through an affine transformation and diffeomorphic Demons [7]. Six first-order texture features were extracted from tumoral and normal tissue. In accordance with previous works [4,5,6], mean signal intensity (M) in both modalities was significantly lower in tumoral tissue ($P < 0.005$ in T2w, $P < 0.0005$ in ADC). Indeed, cellular density in tumoral areas is

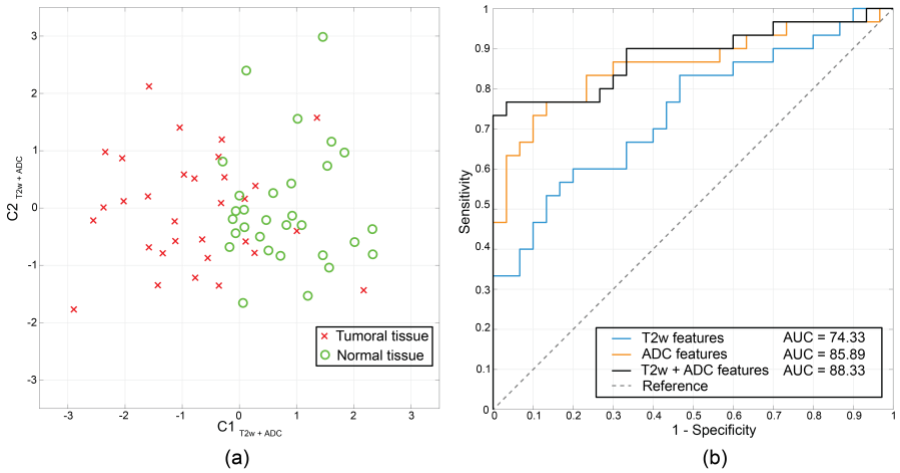

Figure 2. (a) MANOVA scatter plot for T2w + ADC features. (b) ROC curves for T2w, ADC and T2w + ADC features.

higher than normal tissue, hence, these zones appear darker in both T2w and ADC images (see Fig. 1). Anyway, M in ADC led a better discrimination (AUC = 0.85) with respect to T2w (AUC 0.67) as DW imaging is more sensitive to restricted diffusion in tissues. Further, in T2w SD, Ent and H were significantly lower, while no statistical differences of these features were observed in ADC. This leads to the conclusion that differences in heterogeneity between normal and tumoral are more evident in T2w, likely due to its better resolution and therefore its ability to depict tissue microstructure.

Although paired t-test showed an higher number of significant features for T2w, MANOVA analysis revealed that ADC features allows a better separation between normal and cancerous tissue with respect to T2w features (ADC: d = 1, P = 0.0003, AUC = 0.86; T2w: d = 1, P = 0.03, AUC = 0.74). This may be explained from the contribution of M computed in ADC which exhibited the highest AUC equal to 0.85. According to previous research [2,3], combining modalities increased the discrimination between normal and cancerous tissue (d = 1, P = 0.0002, AUC = 0.88), as can be seen in Fig. 2. Surprisingly, the combination of T2w and ADC features allowed to increase the sensitivity from 0.33 (T2w) and 0.47 (ADC) to 0.73 while maintaining the specificity of 1. This aspect could be useful for screening software, where a very high specificity is demanded. Features which mostly contribute to the first canonical variable were: M in ADC (w = 1.3), K in T2 (w = -1.0) and Sk in T2 (w = 0.7). These results suggest that features which do not exhibit a statistical significance when considered alone or within a single modality, may be useful for improving detection when considered in a multiparametric framework. We believe these findings could be useful for researchers which work in the development of CAD system for mpMRI PCa.

Although histogram-based features are not able to describe heterogeneity in terms of spatial patterns as other more advanced textural features are, they have two main advantages: i) robustness respect to the ROI shape and ii) suitability for the analysis of small prostate tumors (< 3 mm) as they can be calculated also in small ROI.

However, two main limitations must be acknowledged: i) only significant PZ lesions were included in the study, limited by the resolution of MR image and ii) selection of the corresponding slices was performed manually and this could be a source of error due to slight slice orientation changes during the specimen cutting. In this regard, we are currently investigating accurate and automatic methods to register the WMH slice to the MR volume.

In future, we will work on extending our population sample, including also MR sequences acquired with different acquisition parameters to evaluate robustness and reproducibility of textural features. Further, we will extend the methodology to transition zone prostate cancer which show different image patterns in mpMRI.

REFERENCES

[1] F. Bray, J. Ferlay, I. Soerjomataram, R. L. Siegel, L. A. Torre, and A. Jemal, "Global cancer statistics 2018: GLOBOCAN estimates of incidence and mortality worldwide for 36 cancers in 185 countries," *CA. Cancer J. Clin.*, vol. 68, no. 6, pp. 394–424, Nov. 2018.

[2] Y. Sun *et al.*, "Multiparametric MRI and radiomics in prostate cancer: a review," *Australas. Phys. Eng. Sci. Med.*, vol. 42, no. 1, pp. 3–25, Mar. 2019.

[3] A. Wibmer *et al.*, "Haralick texture analysis of prostate MRI: utility for differentiating non-cancerous prostate from prostate cancer and differentiating prostate cancers with different Gleason scores," *Eur. Radiol.*, vol. 25, no. 10, pp. 2840–2850, 2015.

[4] E. Niaf, O. Rouvière, F. Mège-Lechevallier, F. Bratan, and C. Lartizien, "Computer-aided diagnosis of prostate cancer in the peripheral zone using multiparametric MRI," *Phys. Med. Biol.*, vol. 57, no. 12, pp. 3833–3851, Jun. 2012.

[5] A. Madabhushi, M. D. Feldman, D. N. Metaxas, J. Tomaszeweski, and D. Chute, "Automated detection of prostatic adenocarcinoma from high-resolution Ex vivo MRI," *IEEE Trans. Med. Imaging*, vol. 24, no. 12, pp. 1611–1625, Dec. 2005.

[6] R. Rozenberg, R. E. Thornhill, T. A. Flood, S. W. Hakim, C. Lim, and N. Schieda, "Whole-Tumor Quantitative Apparent Diffusion Coefficient Histogram and Texture Analysis to Predict Gleason Score Upgrading in Intermediate-Risk 3 + 4 = 7 Prostate Cancer," *Am. J. Roentgenol.*, vol. 206, no. 4, pp. 775–782, Apr. 2016.

[7] B. De Santi *et al.*, "Multimodal T2w and DWI Prostate Gland Automated Registration," in *2019 41st Annual International Conference of the IEEE Engineering in Medicine and Biology Society (EMBC)*, 2019, pp. 4427–4430.

[8] S. Klein, M. Staring, K. Murphy, M. A. Viergever, and J. Pluim, "elastix: A Toolbox for Intensity-Based Medical Image Registration," *IEEE Trans. Med. Imaging*, vol. 29, no. 1, pp. 196–205, Jan. 2010.

[9] V. Giannini *et al.*, "A fully automatic computer aided diagnosis system for peripheral zone prostate cancer detection using multi-parametric magnetic resonance imaging," *Comput. Med. Imaging Graph.*, vol. 46, pp. 219–226, Dec. 2015.